Int. J. Multiphase Flow Vol. 11, No. 4, pp. 445–458, 1985
Printed in the U.S.A.

0301-9322/85 $3.00 + .00
Pergamon/Elsevier

ANALYSIS AND APPLICATION OF SOLID–GAS FLOW INSIDE A VENTURI WITH PARTICLE INTERACTION

EZZAT D. DOSS
Argonne National Laboratory, Argonne, IL 60439, U.S.A.

(*Received* 30 *August* 1983, *in revised form* 8 *September* 1984)

Abstract—A two-phase one-dimensional solid–gas flow model which describes the flow inside a variable area duct has been developed. The model includes multiparticle equations and considers particle–particle interaction. Predictions have been compared with experimental data for the pressure drop and pressure recovery through two venturis at different solid to gas loading ratios. Accurate knowledge of the particle-size distribution is extremely important for good comparison. No meaningful single particle-size diameter is found that yields predictions to agree with the measurements. The venturi may be used as a measuring device for solid–gas flow rates for systems if the particle-size distribution is accurately known. However, the venturi-diffuser section loses its effectiveness in recovering the pressure as the solid loading increases.

1. INTRODUCTION

Monitoring of solid flow rates in the flow of gas–solids mixtures has become increasingly important in many of the chemical and energy-conversion industries for process performance and control where the metering of the gas–solid mixture is a rather important variable in plant operation. Applications include monitoring the feed rate of pulverized coal in feeder lines to furnaces, and coal gasification units and in pneumatic pipelines.

The use of a venturi for metering single phase fluids (gas or liquid) has been thoroughly investigated and standards have been adopted to measure the flow rate with a high degree of accuracy. The challenge is to extend the use of the venturi meter for multiphase flow measurements. The advantages of the venturi for measuring gas–particle suspension flow rates are its simplicity and low cost. A practical problem in applying venturi metering could be plugging of pressure taps. This problem has not been completely solved.

The use of the venturi for flow rate measurements of solids in gas-particle suspensions has been studied experimentally and analytically by several investigators. Carlson *et al.* (1948) investigated the use of nozzle and orifice meter for measuring the flow of air and pulverized coal. Farber (1953) carried out an investigation to determine the behavior of a venturi for metering the solid phase in a gas–solid mixture flowing in horizontal or vertical pipes. Two venturis were used in his experiments and the differential pressure drop and pressure recovery were monitored for different loadings. Sharma & Crowe (1978) and Payne & Crowe (1981) conducted an experimental study to determine the effect of inlet geometry on the differential pressure sensitivity and also the effect of the exit geometry on the pressure recovery of a suspended gas–solids flow in a venturi. Neilson & Gilchrist (1968) investigated the effect of particle size, particle density and initial velocity on the gas–particle motion inside nozzles both analytically and experimentally.

The capability of analytically predicting the flow characteristics of a gas–solid mixture is important for the design and development of many industrial processes and components for energy-conversion systems. Several analytical models have been developed that involve a one-dimensional model of flow behavior through a duct, nozzle or venturi. The early approaches were to assume dynamic and thermal equilibrium between the solid phase and the fluid phase, which corresponds to a single phase, homogeneous fluid with modified properties (Farber 1953, Wallis 1969). However Neilson & Gilchrist (1968) considered that the aerodynamic drag is motion responsible for particle motion but assumed that the particles do not interact with one another or with the duct boundaries. Hogland (1962) presented a summary of different analytical models for gas–particle nozzle flow by many authors. Again particle–particle interaction was not included in these studies. Sharma & Crowe (1978) developed a computational model for a one-dimensional subsonic gas–particle flow using a conservation variable approach over a control volume and treated the coupling between the gas and the particles through the source term concept. In their model the differential equations of the two-phase flow are not solved, rather the basic conservation principles for mass, momentum and energy are directly applied to computation cells. The model does not include particle–particle interaction. The results of their model were compared against the experimental data of Farber (1953) for one venturi geometry.

Recently, Arastoopour *et al.* (1982a), carried out an analysis for pneumatic conveying of solids in a vertical pipe for the purpose of predicting the pressure drop and segregation of particles flowing. Predictions were compared against experimental data and their results indicated that interaction between particles should be considered in the model. Furthermore, in another investigation by Arastoopour *et al.* (1982b), an expression for particle–particle interaction has been developed from experimental data for pressure drop and particle velocity.

In the present work, a one-dimensional two-phase, multiparticle computer model has been developed for gas–solid flow through a variable area duct. In this model particle–particle interaction is included and the differential equations of motion are solved for to yield the gas pressure and velocity, the particle velocity and volume fraction and also the average density of the gas–solid mixture for any particle-size distribution.

The developed model is applied to the geometry of the two venturis considered by Farber (1953). The analytical results for the differential pressure drop between the venturi inlet and the throat and for the pressure recovery between the throat and exit of the two venturis are compared against the experimental data to determine the validity of the model. The sensitivity of the results to particle size, solid to gas loading ratio, and particle–particle interaction has been investigated to assess the accuracy and dependability of the venturi as a measuring device for the solid–gas flow rate.

2. ANALYSIS

The gas–particle flow in a variable area duct is described by a one-dimensional steady-state flow model. Because the gas phase of the flow is considered continuum, the Eulerian system of reference is used to describe the gas variables in the momentum equation. However, the motion of the solid particles, particularly in the dilute phase, is described using the Lagrangian approach. Particle–particle interaction is considered in the particle momentum equation of each species (particle size). Particles are considered in groups, each having the same particle-size diameter.

The set of conservation equations of motion for the gas and the particles is described below.

2.1. *Continuity*

solids:

$$\dot{m}_{p_i} = \phi_i \rho_p u_{p_i} A, \qquad [1]$$

where $i = 1 \cdots n$, which represents a group of particles with a diameter d_i, $\dot{m}$ is the mass flow rate, ϕ the volume fraction, ρ the density, u the velocity and A the cross sectional area. The subscript p refers to the solid particles:

$$\dot{m}_p = \sum_i \dot{m}_{p_i} = \rho_p \sum_i \phi_i u_{p_i} A, \qquad [2]$$

gas:

$$\dot{m}_a = \rho_a \phi_a u_a A, \qquad [3]$$

where

$$\phi_a = 1 - \sum_i \phi_i = 1 - \phi_p. \qquad [4]$$

The subscript a refers to the gas.

2.2. *Particle dynamics*

The force acting on a particle (i) due to collision by a cloud of particles (j) in addition to fluid drag can be written as (Soo 1967)

$$u_{p_i} \frac{\mathrm{d}u_{p_i}}{\mathrm{d}x} = F_i (u_a - u_{p_i}) + \sum_j F_{ij} (u_{p_j} - u_{p_i}) - g, \qquad [5]$$

where x is the direction of motion and g the gravitational acceleration and where

$$F_i = \frac{\text{Drag force due to fluid}}{m_{p_i} \mid u_a - u_{p_i} \mid}$$

and

$$F_{ij} = \frac{\text{Drag force due to collision by } i \text{ particles}}{m_{p_i} \mid u_{p_j} - u_{p_i} \mid}.$$

F is interpreted as the time constant for momentum transfer due to drag force (Soo 1967) where for spherical particles

$$F_i = \frac{3}{4} C_{D_i} \left(\frac{\rho_a}{\rho_p}\right) \frac{\mid u_a - u_{p_i} \mid}{d_i} \qquad [6]$$

and

$$F_{ij} = \frac{3}{2} \eta_{ij} \frac{(d_i + d_j)^2 \mid u_{p_j} - u_{p_i} \mid \phi_j}{d_i^3 \, [1 + (m_{p_j}/m_{p_i})]} \qquad [7]$$

or, in terms of particle diameter

$$F_{ij} = \frac{3}{2} \eta_{ij} \frac{(d_i + d_j)^2 \mid u_{p_j} - u_{p_i} \mid \phi_j}{(d_i^3 + d_j^3)},$$

where η_{ij} is the coefficient of impaction (Soo 1967), C_D the drag coefficient, and m_{p_i} the mass of a particle of species i.

In the above expression for particle–particle interaction, multiple scattering is neglected and the collisions are assumed elastic. Accordingly, and for head-on collision, the coefficient of impaction η_{ij} is taken to be equal to unity by definition (Soo 1967 and Arastoopour *et al.* 1982a). This expression for particle–particle interaction agrees with the trends of the experimental data obtained by Arastoopour (1982b).

2.3. *Gas–particle momentum*

$$\rho_a u_a \phi_a \frac{\mathrm{d}u_a}{\mathrm{d}x} + \rho_p \sum_i \phi_i u_{p_i} \frac{\mathrm{d}u_{p_i}}{\mathrm{d}x} = -\frac{\mathrm{d}p}{\mathrm{d}x} - \frac{4\,\tau_w}{D_h} - [\phi_a \rho_a + \rho_p \phi_p] g, \qquad [8]$$

where p is the static pressure of the gas, τ_w the wall shear stress and D_h the hydraulic diameter.

Equation [8] is reorganized to eliminate the fluid velocity gradient term. By manipulating [1], [2], and [3], [8] becomes

$$\left[1 - \phi_a \frac{u_a^2}{RT}\right]\frac{\mathrm{d}p}{\mathrm{d}x} = \phi_a \rho_a u_a^2\left[\left(1 + \frac{\phi_p}{\phi_a}\right)\frac{1}{A}\frac{\mathrm{d}A}{\mathrm{d}x} + \frac{1}{\phi_a}\sum_i \phi_i \frac{1}{u_{p_i}}\frac{\mathrm{d}u_{p_i}}{\mathrm{d}x}\right] - \rho_p \sum_i \phi_i u_{p_i}\frac{\mathrm{d}u_{p_i}}{\mathrm{d}x} - \frac{4\,\tau_w}{D_h} - (\phi_a \rho_a + \phi_p \rho_p)\, g, \quad [9]$$

where R is the gas constant and T is the temperature of the gas.

In [9], the equation of state for gases is used, where

$$p = \rho_a RT. \quad [10]$$

2.4. *Drag coefficient*

The drag coefficient in [6] between the solid particles and the gas is a function of Reynolds number

$$R_N = \frac{\rho_a \mid u_a - u_p \mid d_p}{\mu_a}, \quad [11]$$

where μ_a is the molecular viscosity of the gas. According to Soo (1967) and Rowe & Henwood (1961)

$$C_D = 0.44 \quad \text{for } R_N \geq 1000 \quad [12]$$

or

$$C_D = \frac{24}{R_N}(1 + 0.15\, R_N^{0.687}) \quad \text{for } R_N < 1000. \quad [13]$$

2.5. *Average density*

The average density $\langle \rho \rangle$ of the solid–gas mixture is defined as

$$\langle \rho \rangle = \sum_i \phi_i \rho_p + \phi_a \rho_a. \quad [14]$$

2.6. *Wall shear stress*

The wall shear stress τ_w is given by

$$\tau_w = \tfrac{1}{2}\, c_f\, \rho_a\, u_a^2. \quad [15]$$

The effect of particle–wall interaction on the skin friction factor may be neglected in the present application because the volume fraction of the solid particles is negligible (<1%) compared to the volume occupied by the gas. However, to be more accurate and account for the presence of solids in the gas, the classical Fanning formula for friction factor for turbulent gas flow is replaced by an equivalent friction factor for the solid–gas mixture according to the results of Pfeffer *et al.* (1966), as follows:

$$(c_{f_{\text{solid-gas}}}/c_{f_{\text{gas}}}) = (1 + X)^{0.3}, \quad [16]$$

where X is the solid to gas mass loading ratio.

Equations [1], [3], [5] and [9] are $2n + 2$ equations (n equations for species mass conservation, n equations for the species particle dynamics, 1 equation for gas mass conservation and 1 equation for the overall momentum equation) for the unknown variables u_a, u_{p_i}, ϕ_i and p where $i = 1$ through n. These equations can be solved by any standard integration routine for a set of ordinary differential equations. A fourth-order modified Runge–Kutta algorithm has been used in our case.

3. RESULTS AND DISCUSSION

In this section, the developed model is applied to the gas–particle flow through a venturi. The predictions are compared with the experimental data of Farber (1953) for two venturis, in both the coverging and diverging sections.

The geometrical details of the two venturis used in the investigation are shown in figure 1. Venturi No. 1 (V-1) has an area ratio = 0.558, whereas the second venturi (V-2) has an area ratio = 0.314. In the experiments, the venturi tubes could be placed either in the horizontal or vertical positions with sufficient approach length. The comparison with the analytical predictions is made for the horizontal configuration.

Powdered alumina-silica catalyst with specific gravity of 2.45 was used in the experiment. The particle-size distribution of the powder, as obtained from a sieve analysis, is shown in figure 2. This particle-size distribution has been divided, in the present analysis, into nine groups. The particle-size and weight percent of each group are as follows:

d_i(μm)	10	25	35	45	60	80	110	150	210
ϕ_i(%)	20	10	10	10	10	10	10	10	10

Four air flow rates (0.0035, 0.005, 0.006 and 0.007 kg/s) were investigated with solid to air mass loading ratios up to 10. Static air pressure at the venturi inlet is taken to be 1.2 atm and air temperature 300 K.

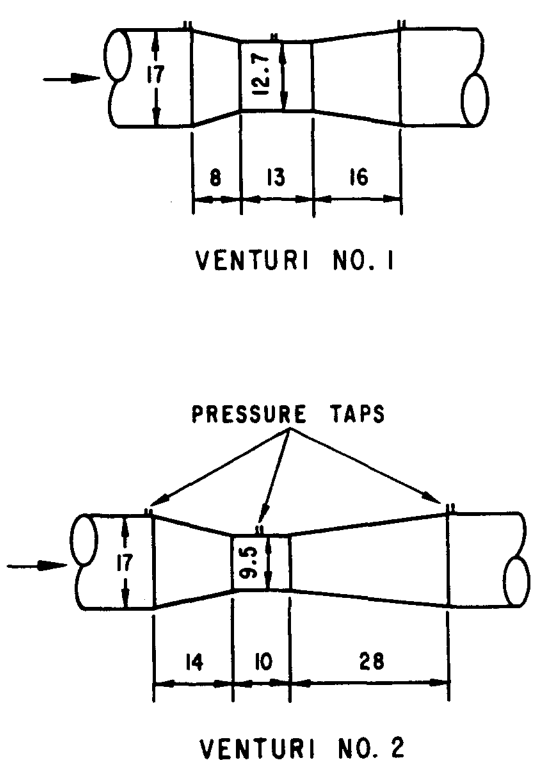

Figure 1. Geometry of two-Venturi meters. (Dimensions in millimeters.)

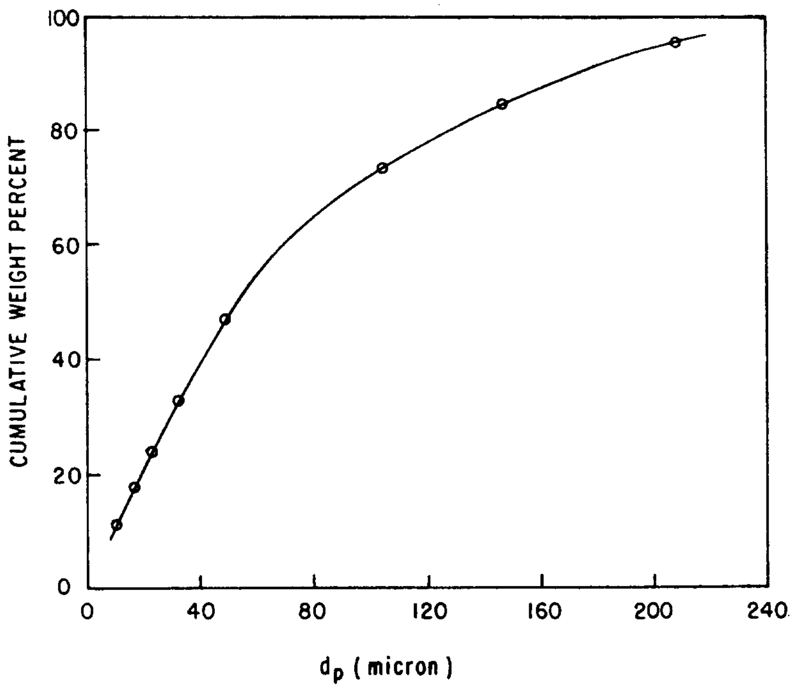

Figure 2. Particle-size distribution.

The velocity of the different size particles at the inlet to the venturi is not known. Therefore, the computations for one case were started a long distance upstream from the venturi, at the point where particles are injected into the gas stream. As expected, the particles accelerated and the small particles approached the gas velocity at the venturi inlet. The computations were repeated starting at the venturi with the assumption that all the solid particles had the same velocity which is equal to 0.99 the gas velocity. Very close agreement was found between the results of the two cases, and therefore for simplicity, this assumption has been used in the applications considered in this work.

The experimental data for the pressure drop through the nozzle and pressure recovery through the diffuser section of the venturi are plotted against the loading (solid to air mass ratio).

3.1. *Effect of particle size on pressure drop*

The pressure drop between the venturi inlet and throat is strongly dependent on the solid particle size and also on the mass flow rate. To influence the pressure distribution in the venturi, the particles should have a relaxation characteristic time smaller than or comparable to the residence time of the gas in the venturi. In this case the solid particles will have sufficient time to exchange momentum and energy with the gas phase while passing through the venturi.

The relaxation time for momentum transfer due to drag force by the gas on the particles (Payne & Crowe 1981 and Soo 1967) is given by

$$\rho_p \, d_p^2 / 18 \, \mu_a$$

and the residence time of the gas in the venturi is

$$D_t / u_a,$$

where D_t is the throat diameter of the venturi. The Stokes number is defined as the ratio between these two characteristic times as

$$ST = \frac{\rho_p d_p^2 u_a}{18 \mu_a D_t}.$$

Therefore if the particles are small, they will have sufficient time to exchange momentum with the gas; thus there will be less lag between the particle velocity and the air stream. In this case it is expected that the smaller the particle size, the larger will be the pressure drop between the inlet and the throat of the venturi. Figure 3 presents the predictions for venturi No. 2 of the variation of the differential pressure drop ratio (with solids/without solids) versus solid to gas loading ratio for different particle sizes. The results indicate as explained earlier, that as the particles get larger, the pressure drop ratio decreases rapidly. One important result observed in figure 3 is the linear dependence of the pressure drop ratio on loading; however the slope of the line is very sensitive to the particle size. For particles 5 μ in diameter or less, the relationship between the pressure drop ratio and solid loading (X) is

$$\Delta P_{G-s}/\Delta P_G = 1 + X.$$

As readily proved from conservation of energy for incompressible flow (Bernoulli equation, ρ = constant), this relationship holds strictly when the velocity of the solid particles is equal to the velocity of the gas. For larger particle sizes, the following empirial relationship is obtained from figure 3:

$$\Delta P_{G-s}/\Delta P_G = 1 + CX,$$

where C is a constant that depends mainly on the particle size. Therefore it is extremely important to include the complete histogram or particle-size distribution in the analysis in

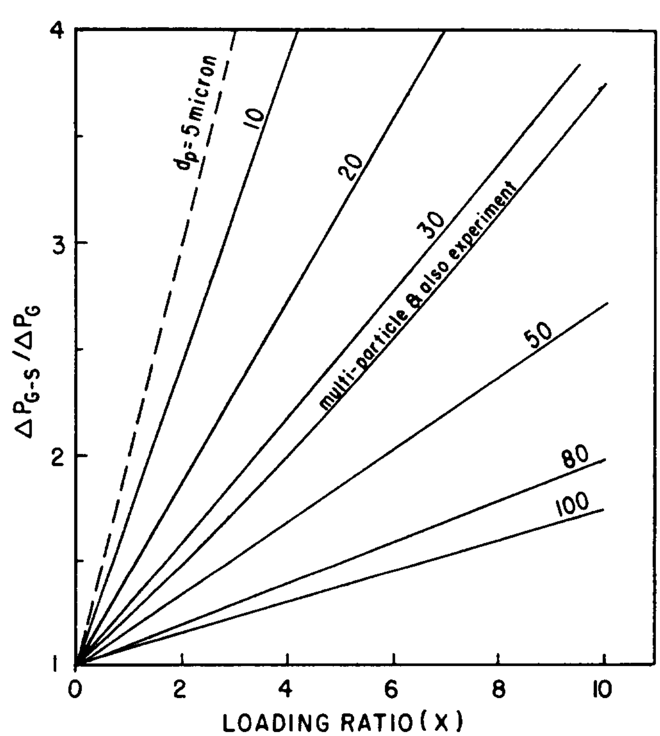

Figure 3. Effect of particle size on pressure drop ratio (venturi No. 2).

order to accurately predict the pressure drop in the venturi due to the presence of solids in the gas.

3.2. *Pressure drop in* V-*1 and* V-*2*

Figures 4 and 5 show a comparison between the theoretical results and the experimental data of Farber for the pressure drop ratio (with and without solids) versus loading for the two venturis. Very good agreement exists between the predictions and the measurements. The measured values of the pressure drop ratio lie far below the asymptotic values corresponding to extremely small particles (<5 μ), and/or to an incompressible, single-phase flow.

An attempt was made to estimate an equivalent single particle-size diameter that yields the same experimental or analytical results obtained with the particle-size distribution shown in figure 2.

An equivalent weight mean diameter equal to 73.5 μ is computed from

$$\langle d_p \rangle_M = \int d_p f_M \, d(d_p),$$

where f_M is the normalized mass distribution function.

The use of this mass mean diameter in the analysis underpredicts the pressure drop measured by Farber as shown in figure 3. The use of a mass-median diameter of about 52 μ (see figure 2) also underpredicts the experimental data.

Alternatively, one can estimate an equivalent mean diameter from

$$\langle d_p \rangle_N = \int d_p f_N \, \mathrm{d}(d_p),$$

where f_N is the number-distribution function. This definition yields a value of 20.6 μ for the average particle diameter which overpredicts the experimental data.

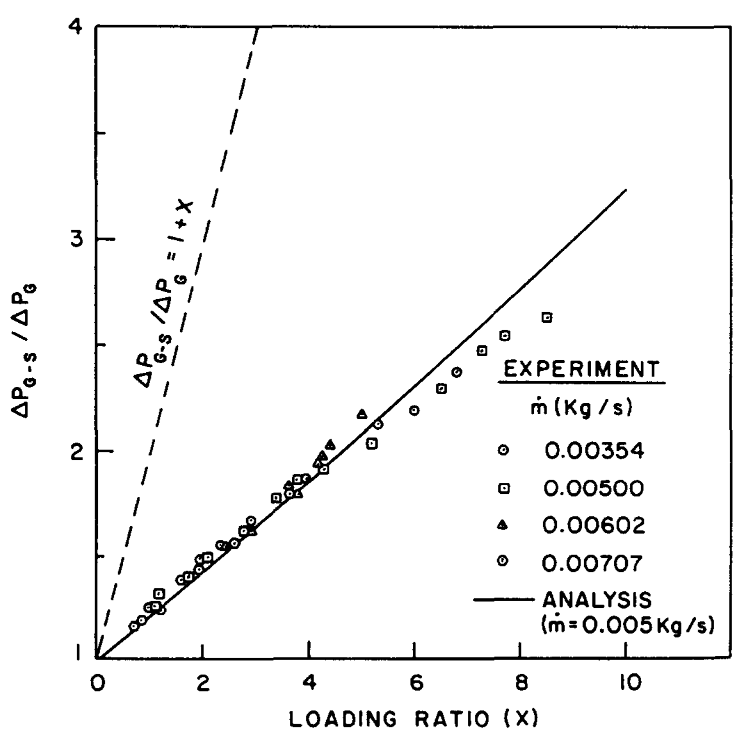

Figure 4. Comparison between experimental data and analysis for pressure drop ratio versus loading for particle-laden and particle-free flows (venturi No. 1).

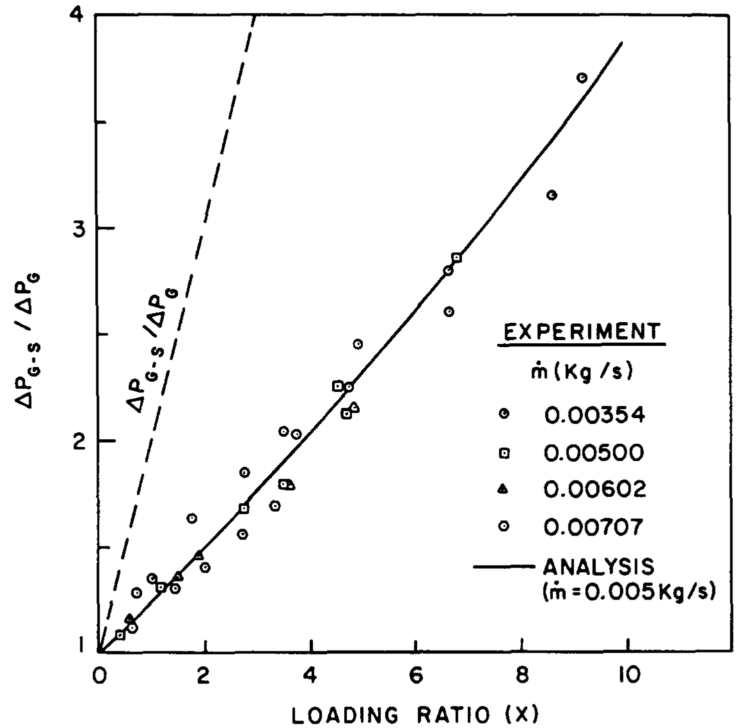

Figure 5. Pressure drop ratio versus loading (venturi No. 2).

Another definition for the mean particle diameter can be based on the cross-sectional area of the particles. This average mean diameter seems more appropriate to use in our application because the drag force between a particle and gas is proportional to this area. In this case the mean particle diameter is defined as

$$\langle d_p \rangle = \int d_p^2 f_N \, \mathrm{d}(d_p).$$

Accordingly, a value of 29.4 μ is calculated for the mean surface diameter. Using this

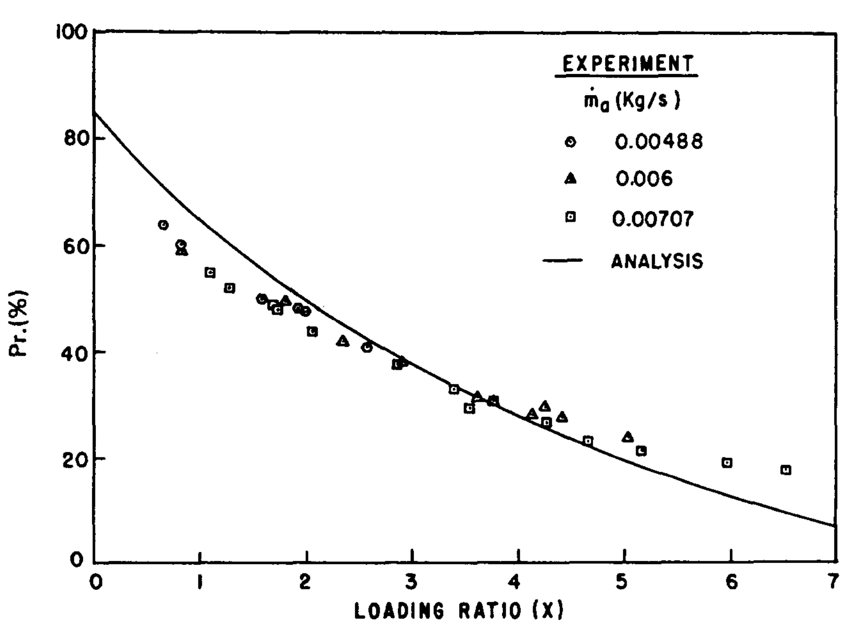

Figure 6. Venturi pressure recovery versus loading (V-1).

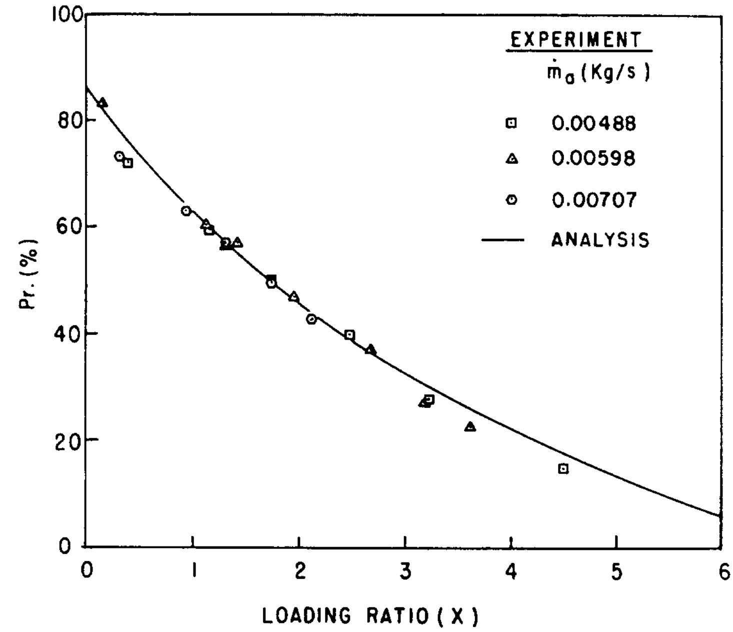

Figure 7. Venturi pressure recovery versus loading (V-2).

average diameter also overpredicts the experimental data; however it yields a better fit than either of the other two definitions for the average diameter.

This exercise confirms the sensitivity of the predictions to the particle size and indicates that there is no reasonable single size particle that may be used to give accurate predictions. This emphasizes the need to include the complete histogram or distribution of the particles in the analytical model, especially the smaller size particles. A similar conclusion was reached by Sharma & Crowe (1978). More strongly, Arastoopour *et al.* (1982a), discussed the flaw in using a mean particle size in a system of wide size distribution and showed that different particle size distributions having the same average particle diameter can generate distinctly different results.

3.3. *Pressure recovery in* V-*1 and* V-*2*

The developed model has been applied also to predict the pressure recovery in the diffuser section of the venturi in the presence of solids in the air stream. Figures 6 and 7 present the experimental and analytical results for the pressure recovery versus solid loading ratio for the two venturis, V-1 and V-2. The pressure recovery ratio (Pr) is defined as the ratio of the pressure recovered in the diffuser section of the venturi to the differential pressure drop between the venturi inlet and the throat. It should be mentioned that in Farber's experiment, individual curves were plotted for the pressure recovery versus solid flow rate for each air mass flow rate. However, it is found that the results fall into a single curve if plotted against the solid to air loading ratio. Good agreement exists between the measurements and the predictions. The results indicate that the venturi-diffuser section may be quite effective in recovering pressure for the cases of no or light solid loadings, but the pressure recovery drops rather rapidly in effectiveness as the solid loading increases.

3.4. *Effect of particle–particle interaction*

In order to investigate the effect of particle–particle interaction on the solid–gas flow characteristics inside the two venturis, the computations were repeated with the omission of the term for particle–particle interaction from the momentum equation [5]. The results for the two venturis showed similar trends. For conciseness, the computational results for the

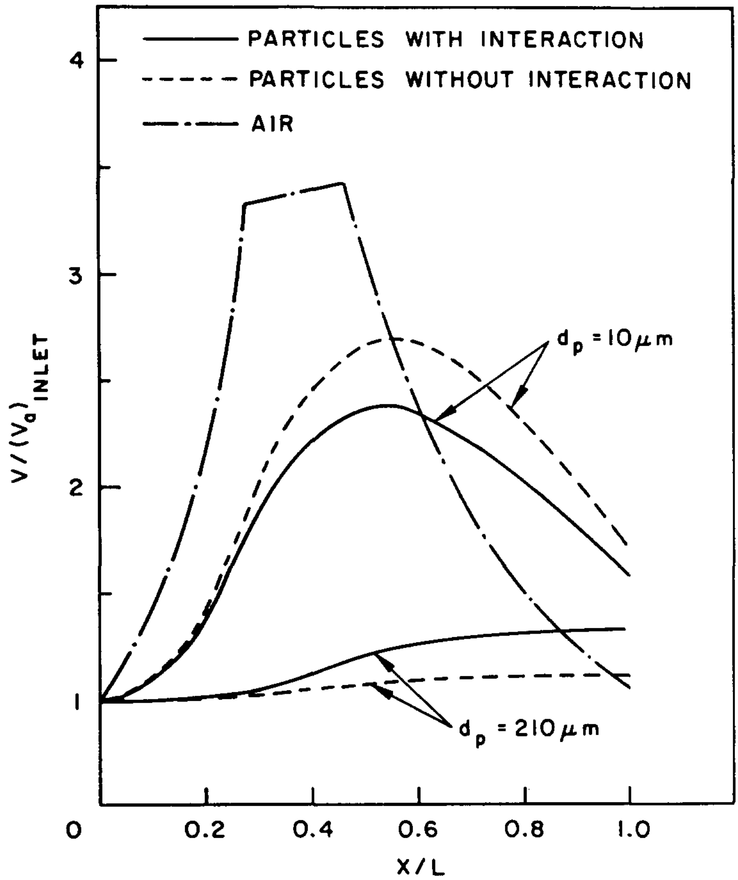

Figure 8. Effect of particle–particle interaction on particle velocity (V-2; loading ratio = 5).

second venturi (No. 2) are presented here because its greater length and smaller throat to the inlet area ratio accentuates the contribution of particle–particle interaction.

Figure 8 presents the nondimensional variation along the venturi of the air flow velocity and the particle velocity for the smallest (10 μ) and the largest (210 μ) size particles considered in the analysis for a solid to air loading ratio equals 5. As expected, the air velocity rapidly increases in the nozzle section, slightly increases in the constant area section, and then rapidly decreases in the diffuser section of the venturi and closely approaches its inlet value. Similarly, the small particles accelerate in the nozzle section; however, they lag behind the air because their Stokes number is somewhat larger than unity. The small particles continue to accelerate because of the drag force, even in the first part of the diffuser section as long as the air velocity is larger than the particle velocity. Later in the diffuser section, the smaller particles decelerate, however at a slower rate than the air. The Stokes number for the largest particles considered is much larger than unity. Therefore, as explained before, their relaxation characteristic time inside the venturi is much larger than the residence time of the gas. Consequently these particles do not accelerate as much as the small particles, rather their velocity stays slightly higher than the inlet value.

When particle–particle interaction is included, the variation of the gas velocity along the venturi remains practically the same because the solids are in a dilute phase. However, the velocity of the small particles decreases, while the velocity of the large particles increases as compared with the results obtained by neglecting particle–particle interaction.

Figures 9 and 10 show the effect of particle–particle interaction on the overall performance of the venturi in terms of the pressure drop ratio (in the nozzle section) and the pressure recovery (in the diffuser section) for different solid to air loading ratios. In general,

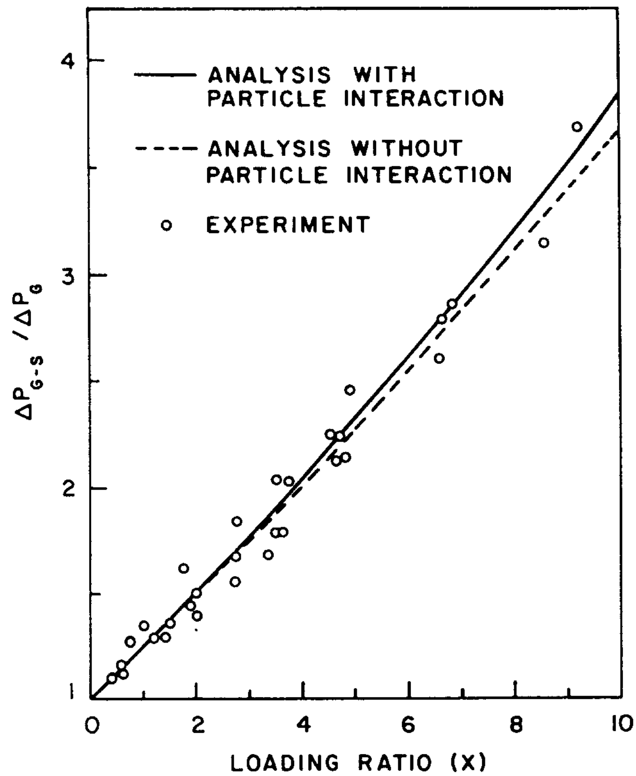

Figure 9. Effect of particle–particle interaction on pressure drop ratio (V-2).

there is a close agreement between the results for the variation of the pressure drop ratio for the two cases with and without particle–particle interaction. However for the case where particle–particle interaction is included, the velocity of the small particles, which contribute the most to the pressure drop, is smaller (see figure 8). This means higher drag force which leads to an increase in the pressure drop in the nozzle section as indicated in figure 9.

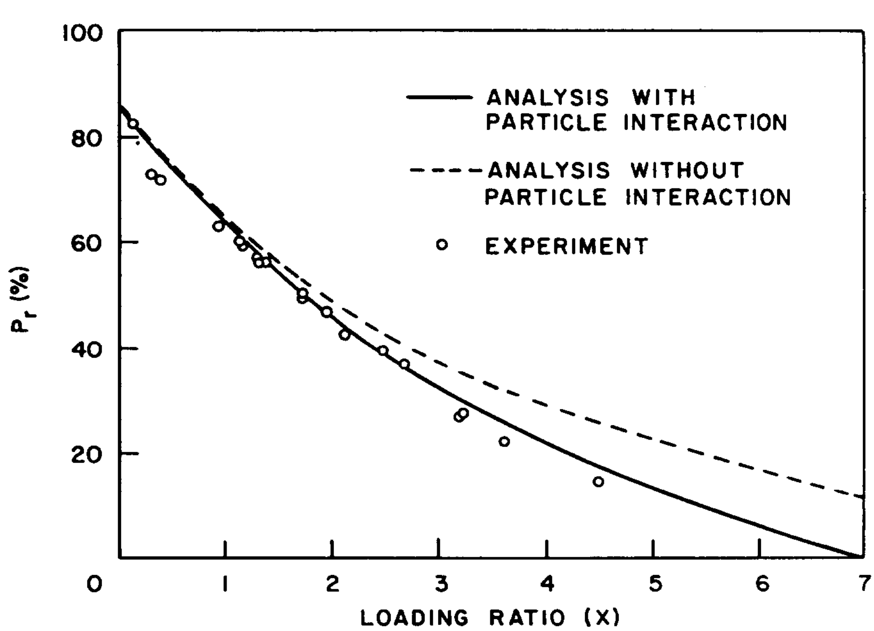

Figure 10. Effect of particle–particle interaction on pressure recovery (V-2).

In the diffuser section of the venturi, higher values for the pressure recovery are predicted for the case of no particle–particle interaction as shown in figure 10. Particle–particle interaction can be viewed as a loss mechanism which leads to a lower diffuser pressure recovery. Therefore, as shown in figure 10, the difference between the results for the two cases (with and without interaction) increases as the loading ratio increases. As a result the predictions for the case of no particle–particle interaction deviates more from the experimental data as the loading ratio increases. This behavior is expected because as the solid loading ratio increases, the probability of collision between particles increases.

The results of this exercise indicates the importance of including particle–particle interaction in the analytical model in order to achieve better and more accurate predictions for the solid–gas flow characteristics inside variable area ducts. Similar conclusions were reached by Arastoopour *et al.* (1982a), in their work on vertical pneumatic conveying of solids.

4. SUMMARY AND CONCLUSIONS

(1) A one-dimensional solid–gas flow model has been developed to describe the flow in a variable area duct. The model includes multiparticle equations and considers particle–particle interaction in the particle–dynamic equation.

(2) The analytical model has been applied to the geometry of two venturis with area ratios of 0.56 and 0.31, and the results are compared with the experimental data of Farber (1953). Good agreement exists between the measurements and the predictions for pressure drop and pressure recovery of the venturi-nozzle and venturi-diffuser sections.

(3) The analytical results show the sensitivity of the venturi pressure drop to the particles size. Therefore the inclusion of the particle-size distribution in the model is extremely important. No meaningful single-particle size diameter has been found that yields predictions to agree with the measurements.

(4) Therefore, in order to use the venturi as a measuring device for solid/gas flow rates, accurate knowledge of the particle-size distribution is required; otherwise frequent calibration of the device will be essential. The venturi may be used to measure the solid flow rate of a system using small particles but it may not be used for measuring the solid flow rates for large particles. The differential pressure drop for the latter case approaches the value obtained with no particles present; i.e, the venturi will not be sensitive to the presence of solids.

(5) Although the venturi-diffuser section is quite effective for pressure recovery of a single phase fluid or with light solids loadings, it loses its effectiveness as the solids loading increases.

(6) It has been demonstrated that it is important to include the particle–particle interaction term in the particle momentum equation in order to achieve better predictions of the solid–gas flow characteristics inside the venturi. Omitting such a term in the analytical model leads to an overprediction of the pressure recovery in the diffuser section of the venturi and the predictions deviate more from the experimental data as the solid to air loading ratio increases.

Acknowledgement—This work was supported by the Department of Energy, U.S. The author thanks Professor S. L. Soo and Dr. K. Porges and Dr. R. Lyczkowski for their technical discussion and suggestions. Also, the author thanks Dr. A. C. Raptis of Argonne National Laboratory and F. Don Freeborn of Morgantown Energy Technology Center for their support and program direction.

REFERENCES

ARASTOOPOUR, H., LIN, S., & WEIL, S. A. 1982a Analysis of Vertical Pneumatic Conveying of Solids Using Multiphase Flow Models. *AIChE. J.* **28**, 467–473.

ARASTOOPOUR, H., WANG, C., & WEIL, S. A. 1982b Particle–Particle Interaction for a Dilute Gas–Solid System. *Chem. Eng. Sci.* **37,** 1379–1386.

CARLSON, H. M., FRAZIER, P. M., & ENGDAHL, R. B. 1948 Meter for Flowing Mixtures of Air and Pulverized Coal. *Trans. ASME* **70,** 65–73.

FARBER, L. 1953 The Venturi as a Meter for Gas–Solids Mixtures. *Trans. ASME* **75,** 943–951.

HOGLAND, R. F. 1962 Recent Advances in Gas–Particle Nozzle Flows. *ARS J.* **32,** 662–671.

NEILSON, J. H., & GILCHRIST, A. 1968 An Analytical and Experimental Investigation of the Velocities of Particles Entrained by the Gas Flow in Nozzles. *J. Fluid Mechan.* **33,** 131–149.

PAYNE, A. L., & CROWE, C. T. 1981 Optimization of the Inlet and Outlet Geometry for Metering Mass Flow of Gas–Solids Mixtures in a Venturi. The Proceedings of the 1981 Symposium on Instrumentation and Control for Fossil Energy Processing, 203–211.

PFEFFER, R., ROSETTI, S., & LIEBLEIN, S. 1966 Analysis and Correlation of Heat-Transfer Coefficient and Friction Factor Data for Dilute Gas–Solid Suspensions. NASA Technical Note, NASA TN D-3603.

ROWE, P. N., & HENWOOD, G. A. 1961 Drag Force in a Hydraulic Model of a Fluidized Bed. *Trans. Inst. Chem. Eng.* **39,** 43–54.

SHARMA, M. P. & CROWE, C. T. 1978 A Novel Physico—Computational Model for Quasi One-Dimensional Gas-Particle Flows. *J. Fluids Eng.* **100,** 343–349.

SOO, S. L. 1967 *Fluid Dynamics of Multi-Phase Systems.* Blaisdell Publishing Co., Waltham, Mass.

WALLIS, G. B. 1969 *One-Dimensional Two-Phase Flow.* McGraw-Hill Book Co., New York.